The 1991 Max Jakob Memorial Award Lecture

Image-Forming Optical Techniques in Heat Transfer: Revival by Computer-Aided Data Processing

F. Mayinger
Lehrstuhl A für Thermodynamik,
Technische Universität,
Arcisstr. 21
8000 Munich 2,
Federal Republic of Germany

Increasing possibilities of computer-aided data processing have fostered a revival of image-forming optical techniques in heat and mass transfer as well as in fluid dynamics. Optical measuring techniques can provide comprehensive and detailed information on the formation of phase interfaces, particle movement, or the size distribution of droplet swarms. Holographic interferograms contain full information, not only about boundary layers restricting transport processes, but also on local coefficients of heat and mass transfer. Laser-induced fluorescence promotes a better understanding of combustion processes by conveying insights into the concentration and the temperature in and around a flame. For describing complicated phenomena in fluid dynamics or in heat transfer by computer programs, global experimental information is not sufficient. Optical techniques provide local data without disturbing the process and with a high temporal resolution. By using the results of optical measuring techniques, it is possible to improve computer programs that describe physical processes. Optical techniques are also very sensitive touchstones for checking the quality of such programs.

1 Holography

1.1 Experimental Method and Optical Setup. Optical methods use changes of light waves as sensoric signals, which are due to interaction between the light and the material. Such changes and interaction consequences include, for example, attenuation, scattering, deflection or reflection and phase shift. Generally one can distinguish between image-forming and non-image-forming methods. Here only the first type shall be discussed.

Recently a new image-forming technique, holography, came into use in studying fluid dynamic processes, and holographic interferometry became a new recording mode for studying temperature fields in boundary layers during heat and mass transfer processes.

The Greek word holography comes from the ability of the method to record the totality (holos) of the light information, respectively of the wave front, namely the amplitude (as brightness), the wavelength (as color), and the phase position of the light. Holography demands a source emitting coherent light. For the general theory of holography, reference is made to the literature (Kiemle and Röss, 1969, Smith, 1969; Caufield and Lu, 1971). Here only some principles necessary for understanding the holographic measurement techniques are mentioned. In Fig. 1 the holographic two-step image-forming process of recording and reconstructing an arbitrary wave front is illustrated.

The object is illuminated by a monochromatic light source and the reflected or scattered light falls directly onto a photographic plate. This object wave usually has a very complicated wavefront. According to the principle of Huygens, one can, however, regard it to be the superposition of many elementary spherical waves. In order to simplify the matter, only one wave is drawn in Fig. 1. A second wave, called "reference wave" is superimposed on the first. If the waves are mutually coherent, they form a stable interference pattern when they meet on the photographic plate. This system of fringes can be recorded on the photographic emulsion. After the chemical processing of the plate, it is called "hologram." The amplitude is recorded in the form of different contrast of the fringes and the phase in the spatial variations of the pattern.

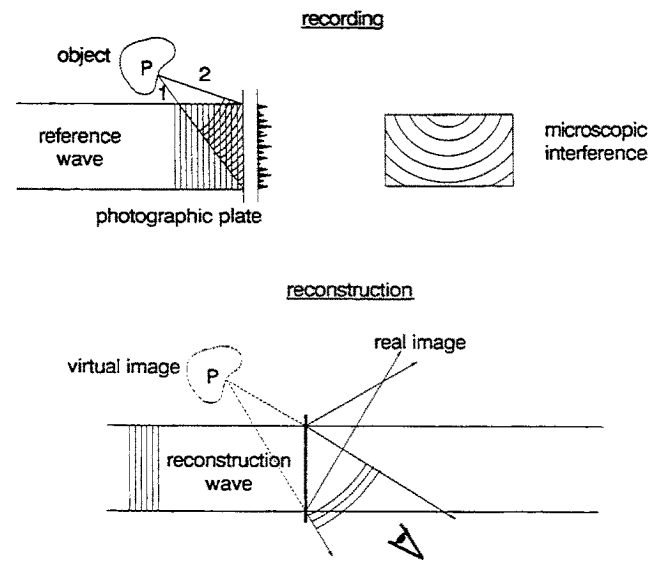

Fig. 1 Principle of holographic two-step image-forming process

If the plate is subsequently illuminated by a light beam similar to the original reference wave, the microscopic pattern acts like a defraction grating with variable grating constant. The light transmitted consists of a zero-order wave, traveling

Contributed by the Heat Transfer Division and presented at the ASME National Heat Transfer Conference, San Diego, California, August 9–12, 1992. Manuscript received by the Heat Transfer Division April 1993; revision received August 1993. Keywords: Flow Visualization, Measurement Techniques. Technical Editor: R. Viskanta.

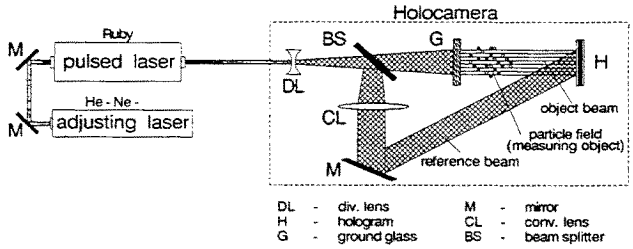

Fig. 2 Holographic setup for ultrashort time exposures with a pulsed laser

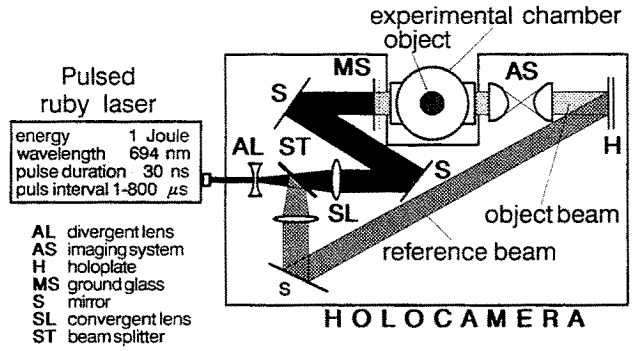

Fig. 3 Holographic interferometer for spray analysis

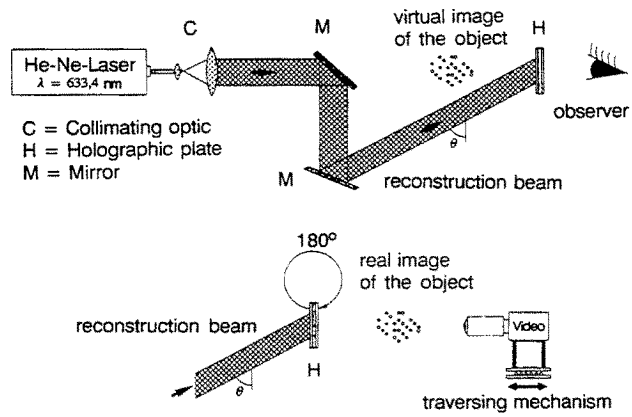

Fig. 4 Optical arrangement for the reconstruction of pulsed laser holograms

in the direction of the reconstructing beam, plus two first-order waves. One of these first-order waves travels in the same direction as the original object wave and has the same amplitude and phase distribution. The first-order wave produces a virtual image in front of the holographic plate, seen from the side of the incoming reference beam. The other wave goes in the opposite direction and creates a real image of the object behind the photographic plate. This real image can be studied with various reconstruction devices, such as a microscope.

For conventional applications of holography, one can use lasers emitting continuous light, for which adjustment of the holographic plate is a trivial task. The recording of very fast moving or changing objects needs ultrashort exposure times, which can be achieved by using a pulsed laser, for example, a ruby laser with pulse durations of 20–30 ns. A holographic setup using a pulsed laser is shown in Fig. 2. For adjusting such a holographic setup with a pulsed laser, one needs a second laser emitting continuous light to adjust the holographic arrangement and the photographic plate. With a ruby laser as a light source, one can use the special feature of the ruby crystal to transmit red light. The beam of a helium-neon-continuous laser can be arranged in such a way that it travels through the ruby of the pulsed laser. The holographic setup shown in Fig. 2 is a special arrangement for studying particle flow or phase distribution in multiphase mixtures. It presents a very suitable nonintrusive method to visualize dispersed flow with particles or droplets not smaller than 10 λ where λ is the wavelength of the laser light.

A more sophisticated arrangement for recording pulsed laser holograms is shown in Fig. 3. In this arrangement the light emitted by the pulsed ruby laser travels through a lens and mirror system, where it is expanded, divided, and guided through the measuring object and onto the holographic plate. The laser beam is first expanded in the lens AL and then divided in the beam splitter ST to produce the object beam and the reference beam. The object beam travels via a collecting lens, two mirrors, and a screen through the object, and after the object passes an imaging lens before it falls onto the holographic plate. There it is superimposed by the reference wave, which is split off by the beam splitter ST and falls via the collecting lens SL and a mirror onto the holographic plate, bypassing the object. An instantaneous picture of the situation in the spray can be registered. If the electronic system of the ruby laser emits more than one laser pulse within a very short period of time, sequences of the spray behavior can be stored on the photographic emulsion of the holographic plate, from which the velocity of the droplets as well as their changes in the size and geometric form can be evaluated. The evaluation, however, needs a very sophisticated and computerized procedure, which will be briefly described later.

For evaluating the hologram, it first has to be reconstructed as demonstrated in Fig. 4. As an example, the formation of a droplet spray leaving a nozzle is studied in this reconstructing procedure. After chemical processing, the holographic plate is replaced in the old position and then illuminated by a continuously light-emitting helium–neon laser. The new beam produced by this laser is now called a reconstruction beam. If the holographic plate is replaced in the same orientation it had when the exposure was made, one can look at it with the naked eye and see a virtual image of the droplet spray exactly at the place where it was produced previously. For a quantitative evaluation one needs a closer examination via an enlarging lens or a microscope and by a camera, perferably a video camera. To do this, the holographic plate has to be turned by 180 deg, when positioning to the old place. By illuminating with the reconstruction beam, a real image of the spray is now produced, which has a three-dimensional extension. The arrangement of the video camera is shown in Fig. 5. For technical evaluation, the camera is focused to the midplane of the spray image. The camera is moved forward or backward with a fixed focus of the lens so that the spray cloud can be evaluated plane by plane.

1.2 Computer-Aided Evaluation. The quantitative evaluation via the video camera works with a computer system. The main components of this system are a digitizer, a graphic monitor, and a PC. The video camera is scanning the real image of the reconstructed hologram O and sends its information to the digitizer D. It changes the electrical signal from an analog character to a digital one, and stores it in a frame memory. Now the computer C can use the digitalized information for performing the image reprocessing.

The processing of images obtained from holograms involves:

- separation of the droplet images from the background.
- identification of sharply focused droplets.
- measuring of their projected areas.
- evaluation of their equivalent diameters and center points.

By applying an average filter, the noisy background can be suppressed. Afterward the sharply focused parts of the image have to be identified. This can be realized by contouring the parts of the image. It is obvious that sharply focused contours deliver a strong grey gradient and out-of-focus images have a

smooth transition of grey values. To identify the well-focused contours, many so-called auto-focus-algorithms have been developed (Lighthart and Groen, 1982). The gradient of the grey values represents a criterion to separate sharply focused parts of an image from unsharply focused ones. This can be done by using a Sobel operator. Strong gradients are enhanced while weak ones tend to disappear. The last step is to eliminate all particles that are not well focused. This can be done by allowing only pixels to remain in the image, which have a grey gradient to their neighbors above a certain value. For details, reference is made to the work by Chavez and Mayinger (1990). By this procedure a "picture" is electronically produced containing only contours, which are within a very narrow tolerance of the focusing plane.

It may happen that the contours of some parts—for example, droplets—do not have a closed and continuous outline, because pixels may have been extinguished spotwise during the gradient checking procedure. Therefore, a next step has to follow, in which the open contours are filled with color to produce closed outlines of the particle reproductions. In order not to create new spots by this process, the situation after the contouring is compared with that which existed before the out-of-focus particles were eliminated. A "particle" in the new picture is only accepted if it existed already in the original picture. Finally, the remaining particle reproductions are filled with color and now the evaluation with respect to particle size, form, and concentration can go on.

After this plane in the hologram has been evaluated, the video camera is moved slightly and the whole procedure starts again. So the picture can be evaluated plane by plane and a three-dimensional picture can be reconstructed.

An example of a computerized reproduction of the veil and the droplet swarm originating from a nozzle is shown in Fig. 6 (Chavez and Mayinger, 1990, 1992). It conveys a good impression of how the information of a hologram can be improved by computerized evaluation. While the photograph and the left-hand side of this figure show only the shape of the veil, the computerized picture on the right-hand side clearly presents the thickness of the liquid film of the veil and also shows its wavy nature. In addition, the droplets separating from the lower end of the veil are clearly defined.

A sequence of reproduced "pictures" by this computer-aided image processing is shown in Fig. 7. The upper row in this figure shows the region of a spray near the nozzle and the lower one a region further downstream where the veil already is disintegrated into a droplet swarm.

1.3 Double Exposure Technique. If two exposures of a droplet spray are illuminated onto the same holographic plate within a short time, the velocity of the droplets can also be determined from such a hologram (Chavez and Mayinger, 1992). To evaluate such a double-exposed hologram, first the

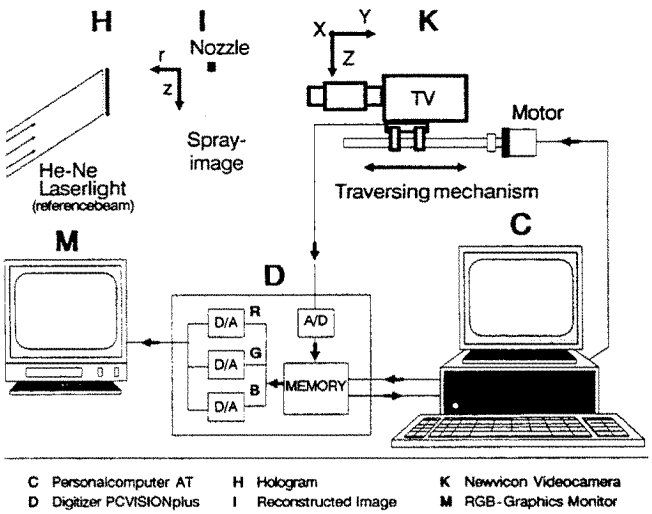

Fig. 5 Digital image processing system for the evaluation of pulsed laser holograms

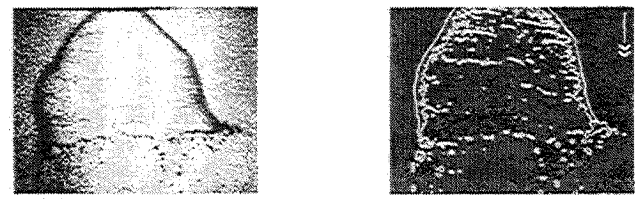

Fig. 6 Veil and spray flow behind a nozzle: left side: photographic view, right side: evaluation of a hologram

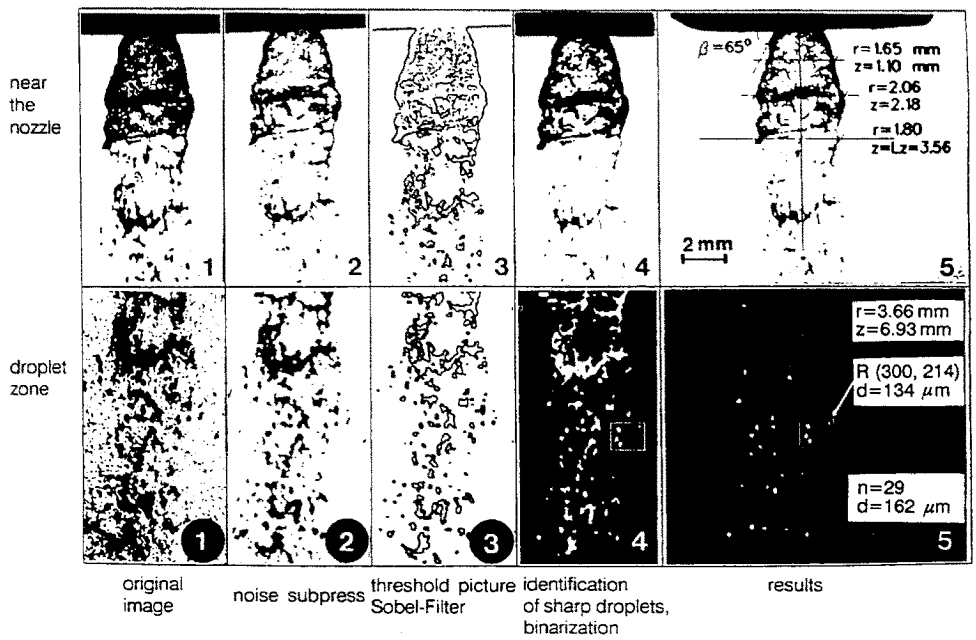

Fig. 7 Steps of image-processing of a hologram: upper row: spray near the nozzle; lower row: spray downstream of the nozzle

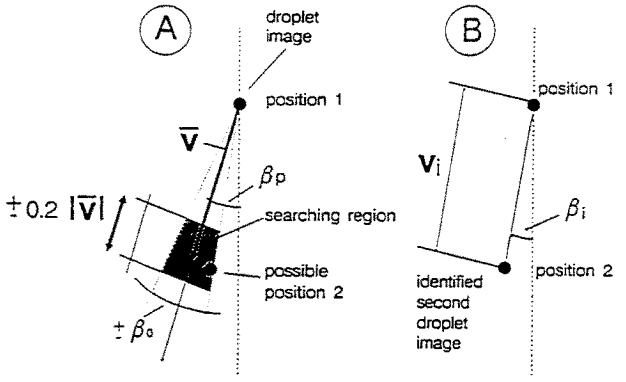

Fig. 8 Method for evaluating particle velocity from double pulse holograms; definition of the search area

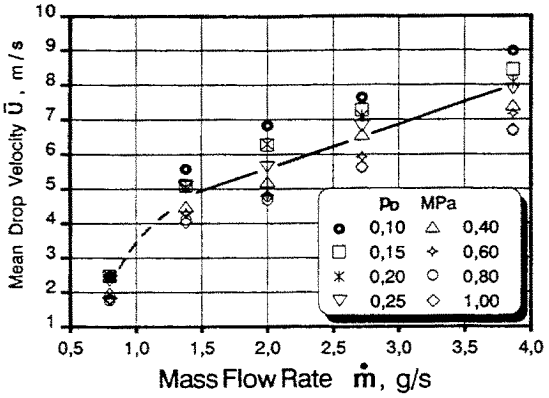

Fig. 9 Mean droplet velocity in a spray as a function of flow rate at different ambient pressures

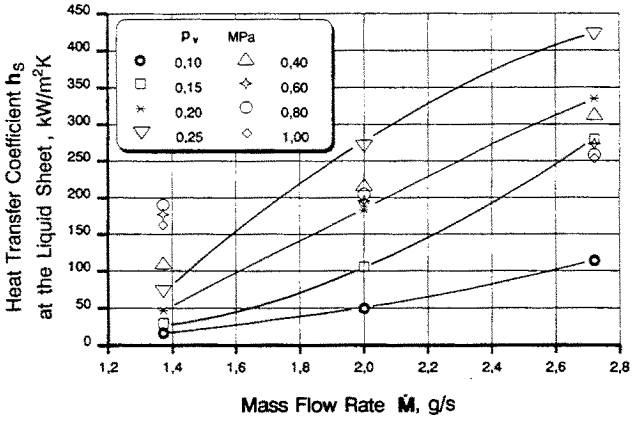

Fig. 10 Heat transfer coefficient during condensation at the phase interface of liquid droplets and vapor

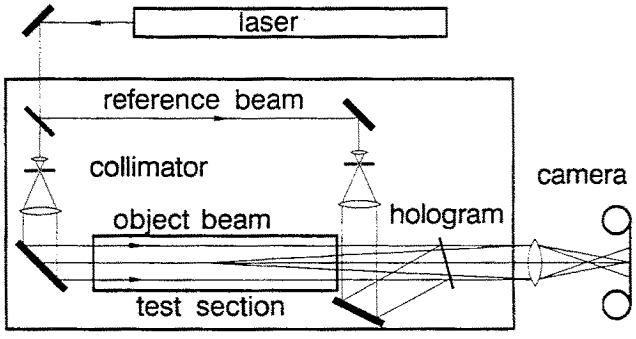

Fig. 11 Optical setup for holographic interferometry

same procedure has to be performed as briefly discussed before. After that the center point of each droplet has to be defined by the computer, which is the basis for determining the distance between the two images of the same droplet, and for evaluating the velocities and trajectories of the droplets. In the next step, the computer draws connection lines between all portrayed particles, regardless of whether they originate from the first or the second exposure. These connecting lines are evaluated with respect to direction and length via a Fourier analysis. This Fourier analysis converts the spatial distribution into a normalized frequency distribution with the maximum F_{max} used as a norm. With this information a second Fourier transformation with the distance as the independent variable is carried out. The preferential angle and the preferential distance appear as peaks in the Fourier diagram, showing the main direction and the mean velocity of the droplets.

In the next step, the computer defines a searching area in a spatial distance from each particle portrayed with this information as briefly sketched in Fig. 8. If it finds the image of a particle within this searching area, it defines it as the second exposure of the particle at position 1, and it calculates the real velocity V_i and the direction β_i of the droplet. If it does not find a particle image within this searching area, it cancels the input of position 1, assuming that the particle moved out of the focused plane before the second exposure was done. In a more sophisticated way, this searching procedure can be also performed between two or more focus planes. This step, however, is very time consuming on the computer.

The data produced by this opto-electronic process are of high accuracy, as Fig. 9 demonstrates. The suspicion that the computerized processing of the double exposure hologram produces a large scattering in the velocity data is misproved by this figure. Even the influence of the pressure of the atmosphere, in which the droplets are traveling, is clearly brought out.

If the droplets are moving in a vapor atmosphere of the same substance as the liquid, and if the temperature of the liquid is below the saturation temperature, condensation occurs at the phase interface, which makes the volume of the droplet grow. This increase in diameter can also be depicted from double-exposure holograms and evaluated by the computer. By using a simple energy balance, the condensation heat transfer can be calculated from this growth of volume versus time. The accuracy and the reproducibility of the described opto-electronic measuring technique are good enough to determine the heat transfer coefficients at the veil and at the droplet cloud, as Fig. 10 demonstrates. The heat transfer data are averaged values from all droplets being reproduced in a hologram.

2 Holographic Interferometry

2.1 Principal Arrangement of Optical Components. By using the recording capabilities of holography, different waves—even those shifted in time—can be stored on the same holographic plate. By illuminating the developed holographic plate with the reference wave, all object waves are reconstructed simultaneously. Where they differ only slightly from each other, they can interfere with each other. These are the fundamentals of holographic interferometry.

In heat and mass transfer, the temperature and the concentration distribution in a fluid are of special interest. To investigate such processes, a so-called through light method is used, where the object wave is irradiating through a volume, in which heat or mass transport takes place.

An exemplary arrangement for holographic investigations is shown in Fig. 11. A beam splitter divides the laser beam in an object wave and in a reference wave, which is also called

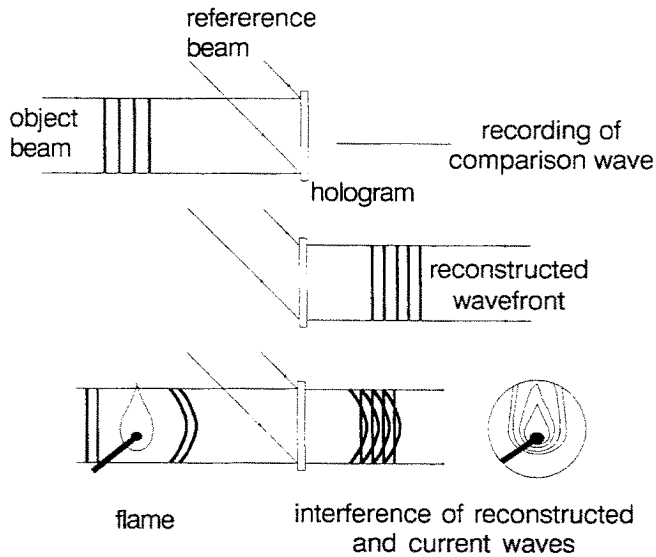

Fig. 12 Real-time method for holographic interferometry

a comparison wave. Both waves are expanded to parallel wave bundles behind the beam splitter via lenses, usually consisting of an arrangement of a microscope lens and a collecting lens. The expanded and parallel organized object wave travels through the space with the research object of interest—called a test section—in which the distribution of temperature or concentration may be measured. The reference wave bypasses the test section and falls directly onto the photographic plate.

To obtain a well-focused picture of a hologram, the interference pattern between the object and the reference wave must be completely stable. With longer exposure times, by using a continuous laser, the optical components have to be mounted on vibration-free tables. On the other hand, there is no need for a high optical quality of the optical components—as it is the case in conventional interferometry—because only relative changes of the object wave are recorded, and optical errors are automatically compensated by the interferometric method. In many cases, only a two-dimensional temperature distribution over a test object is of interest, and it is then good enough to record the change of the refractive index only in a two-dimensional way. For such cases object waves with parallel light provide pictures of high quality. There are many possibilities for arranging the optical setups to form a holographic interferometer, which cannot be discussed here in detail. Reference is, therefore, made to the literature (Mayinger and Panknin, 1974; Mayinger, 1991).

Several procedures exist to produce interferograms; here only one method will be explained, which can also be used in connection with high-speed cinematography. It is called a "real-time-method," because it observes a process to be investigated in real time and continuously. The method is illustrated in Fig. 12.

After the first exposure, by which the comparison wave is recorded and during which no heat transfer is going on in the test section, the hologram is developed and fixed. Remaining at its place or repositioned accurately, the comparison wave is reconstructed continuously by illuminating the hologram with the reference wave. This reconstructed wave can now be superimposed onto the momentary object wave. If the object wave is not changed, compared to the situation before the chemical developing process, and if the hologram is precisely repositioned, no interference fringes will be seen on the hologram.

Now the heat transfer process and boiling or condensation for two-phase flow can be started. Due to the heat transport, a temperature field is formed in the fluid, and the object wave receives an additional phase shift, when passing through this temperature field. Behind the hologram, both waves interfere with each other, and the changes of the interference pattern can be continuously observed or photographed.

The real-time method demands an accurate reconstruction of the comparison wave. Therefore, the hologram must be repositioned precisely at its original place. This can be done by using an adjustable plate holder, which can be purchased from the market. It is recommended to use a plate holder, where the final adjustment can be done via remote control, for example, with quartz crystals. The adjustment of the repositioned holographic plate gets its feedback control signals on an optical basis, because the adjustment has to be done in such a way that the interference fringes—at first visible due to nonprecise position of the plate—disappear during this procedure. This, certainly, has to be done without the heat transfer process having started. However, the same pressure and temperature exist in the fluid, under which the system is operated during the experiments.

A series of holographic interferograms taken with this method is illustrated in Fig. 13, where the boundary layer and the bubble formation at a heated horizontal surface, immersed in water, flowing slowly from the right to the left, was studied. The bulk temperature of the water was slightly below the saturation temperature and, therefore, the bubble is condensing after penetrating the superheated boundary layer near the wall. The black and white fringes in Fig. 13 represent lines of constant temperature in a first approximation. From this figure we can also learn something about the limitation, with which this and all other interferometric methods are afflicted. The temperature field in the fluid near the heated wall is not only shifting the phase of the light wave, it is also deflecting the light beam when traveling through it. This deflection has the consequence that with very high temperature gradients at the wall—as is the case in subcooled boiling—the zone immediately adjacent to the wall cannot be seen. With lower heat fluxes, this deflection is not a problem in interferometry.

The evaluation of the interference fringes and the derivation of the temperature field from the interference pattern as well as the calculation of the local heat transfer coefficients or the Nusselt numbers is the same as with the conventional interferometry, for example, the Mach-Zehnder-interferometry, and is well described in the literature (Hauf and Grigull, 1970; Hauf 1991). Therefore, the optical rules and the mathematical procedure are not presented here. Also the evaluation of spherical and cylindrical temperature fields by using the Abel correction can be found in the literature (Hauf and Grigull, 1970; Chen, 1985).

Evaluating a holographic interferogram by hand, as was done until a short time ago, was a very time consuming and tedious task. Today computerized evaluation is available, which reduces the time needed for deducing the local Nusselt numbers out of an interferogram from several hours down to a few seconds. For computerized evaluation one needs the same components as described in the chapter before, namely a video camera, a digitizer, a graphic monitor, and a PC. In the first step the procedure is very similar to that explained in Section 1. Also searching the gradients of greyness is similar, as briefly mentioned before. Then, however, a special algorithm has to be used to enhance the contrast of the grey steps to find the maximum of the greyness and to formulate the contour of the heat transferring wall in a digital way on the computer. Knowing the greyness maxima of the interference fringes and the digitized contour of the wall, one can determine the exact distances of the interference fringes—and by this of the isotherms—in the boundary layer near the wall. Isotherms usually run normal to the heat flux, and so knowing the position of the isotherms, one gets the temperature gradient orthogonal to the wall. By assuming sticking conditions at the wall, one can derive the local heat transfer coefficient from this tem-

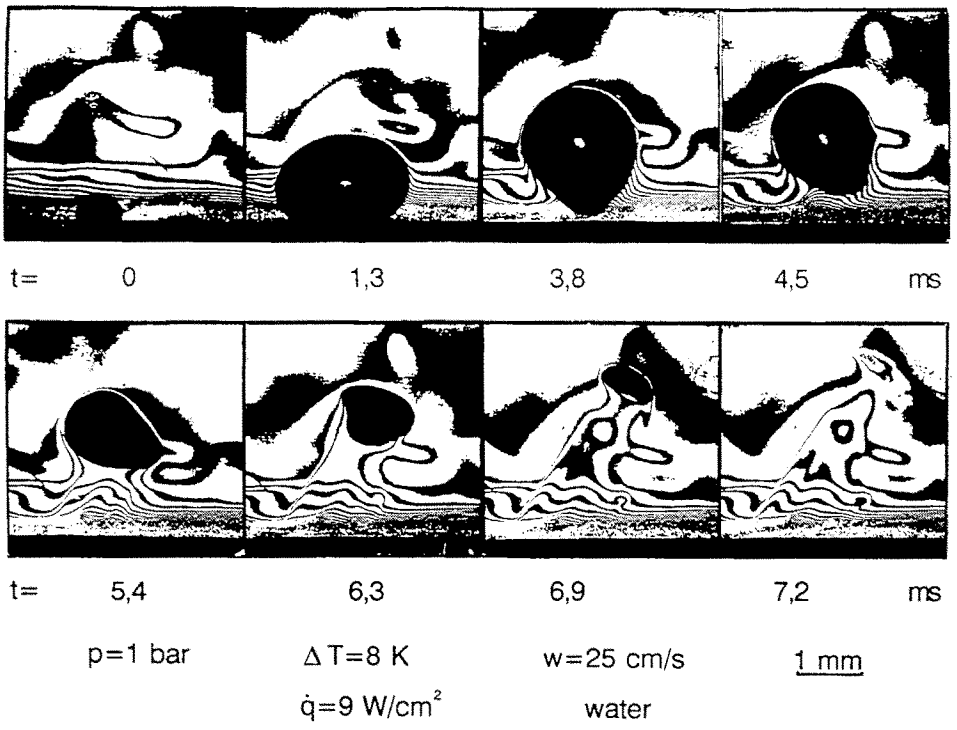

Fig. 13 Interferograms of subcooled boiling on a heated wall

perature gradient. For studying these various algorithmic procedures in detail, reference is made to a thesis by Klas (1993).

Here only the result of such a computerized evaluation will be briefly discussed as an example. Figure 14 shows the interference fringes and the local Nusselt numbers around an element of a compact heat exchanger designed for application in aviation at high altitudes with low atmospheric density. The computer automatically draws lines perpendicular to the surface of the heat transfer element and also lines of constant Nusselt numbers parallel to the surface of the heat transfer element. From the interference fringes it then calculates the local Nusselt numbers at each position of the element.

With very high heat transfer coefficients, the boundary layer at the wall usually becomes very thin, down to a few hundredths of a millimeter. In this case, it is difficult to evaluate the interference pattern if it is registered with the procedure described up to now. A slightly altered method, the so-called "finite fringe method," offers some benefits. In this method, after the reference hologram was produced, a pattern of parallel interference fringes is created by tilting the mirror in the reference wave of Fig. 15, or by moving the holographic plate there within a few wavelengths. The direction of the pattern can be selected as one likes, and it is only depending on the direction of the movement of the mirror or of the holographic plate.

This pattern of parallel interference fringes is then distorted by the temperature field due to the heat transfer process. The distortion or deflection of each fringe from its original parallel directions is a measure from the temperature gradient at this place and allows us to deduce the heat flux and by this the heat transfer coefficient.

Figure 16 demonstrates the possibilities of using these techniques in a flow with a bubble condensing in a liquid. By combining this method with high-speed cinematography, it allows an inertia-less and precise evaluation of the heat transfer coefficient at the phase interface of the condensing bubble. Holographic interferometry, certainly, can only be used if the flow situation is not too complicated and if the bubble population is not too numerous so that individual bubbles can be identified. It is not possible to look inside the bubbles, because the light is totally reflected at the phase interface.

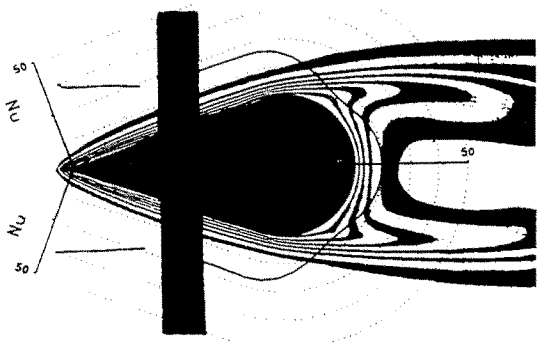

Fig. 14 Interferogram and local Nusselt numbers around a heat transfer element of a compact heat exchanger

2.2 Two-Wavelengths Method. The phase shift of the light wave when traveling through a gas or liquid is a function of the change in the density of the fluid. In pure substances the density depends only on temperature and pressure. In multicomponent systems the concentration also influences the density. Conventional interferometry, whether according Mach-Zehnder or on a holographic basis, works on the assumption that the alteration of the density is affected by a temperature change only. If variations in the refractive index are caused not only by a temperature, but also by a concentration change, this simple evaluation method is no longer possible. There is, however, a method to determine simultaneously the temperature and the concentration field by optical means, which was first proposed by El-Wakil et al. (1966), and which was further developed by Panknin (1977) and Panknin and Mayinger (1978) to the so-called "two-wavelengths holographic interferometry." It is performed by applying the dependence of the refractive index on the wavelength of the light. The problem

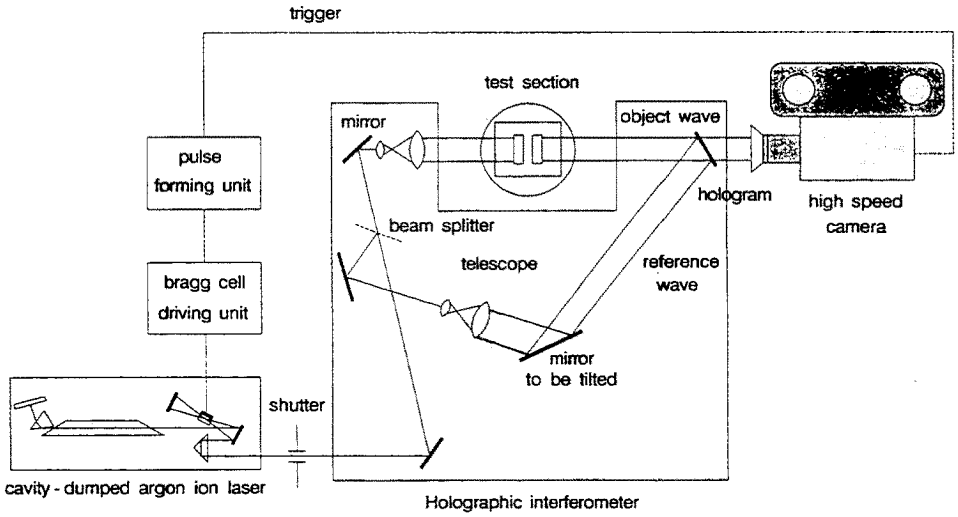

Fig. 15 Finite fringe method for holographic interferometry

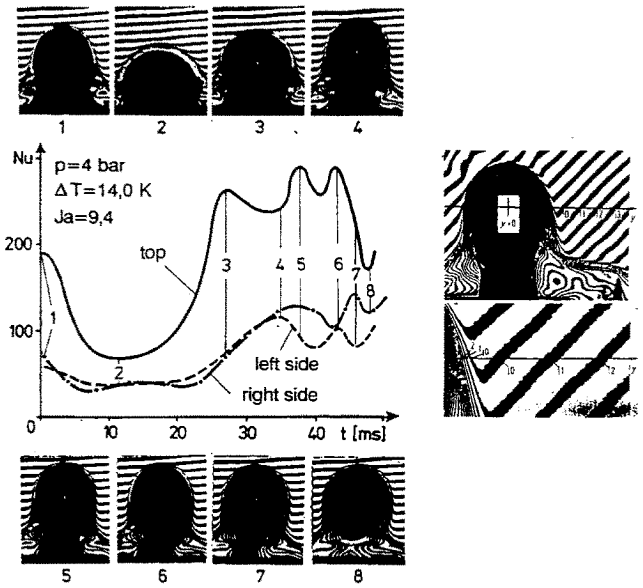

Fig. 16 Heat transfer at the phase interface of a vapor bubble condensing in a subcooled liquid, deduced from a sequence of interferograms

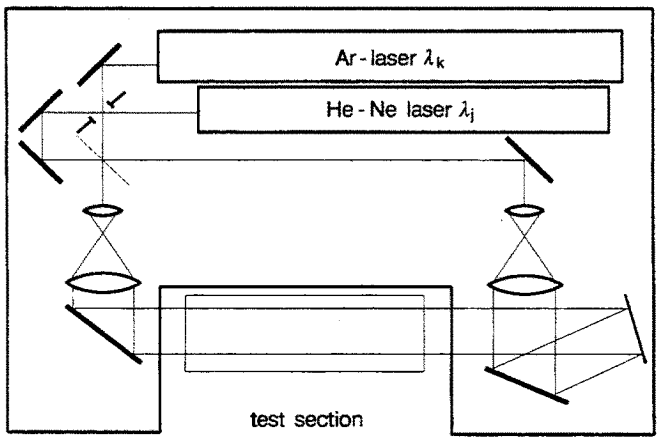

Fig. 17 Optical arrangement for holographic two-wavelength interferometry

with this two-wavelengths interferometry is that the two interferograms originating from these two beams of different wavelength have to be superimposed very accurately. Here, the peculiarity of the holography allowing the recording of different interference pattern on one and the same plate is a great help to overcome these difficulties. A simple setup for the holographic two-wavelength interferometry is shown in Fig. 17. It resembles very much the arrangement of Fig. 11, and actually the only difference is that two lasers are used as light sources, a He-Ne laser emitting red light, and an argon laser emitting green light. The two beams intersect, and at the position of this intersection a shutter is placed, which guarantees equal exposure times for both waves. The beams are then superimposed by means of a beam splitter, which results in two object and two reference waves at different wavelengths.

For the evaluation of the interferograms, some simple equations shall be presented. For a more detailed study, reference is made to the work by Panknin (1977). In an ideal gas, the Boyle-Mariott law is valid and the relation between fringe shift and temperature and concentration distribution can be easily formulated by

$$S(x, y)\lambda = \frac{3pl}{2R} N_m \left[\frac{1}{T(x, y)} - \frac{1}{T_\infty} \right] \tag{1}$$

In this equation S is the multiple of a wavelength, and l is the length of the test section, in which the refractive index is varied. R and p stand for the gas constant and the absolute pressure, respectively. The molar refractivity N_m of a mixture of two gaseous components is given by

$$N_m = N_a C_a + N_b C_b; \text{ with } C_a + B_b = 1 \tag{2}$$

where N_a and N_b are the molar refractivities of the components and C is the concentration of the component in the mixture. During recording of the comparison wave, the temperature distribution T in the test section is constant, and there are only two components of the mixture.

Combining Eqs. (1) and (2), we obtain for each wavelength

$$S(x, y)\lambda = \frac{3pl}{2R} \left[\frac{1}{T(x, y)} \left(N_a + C_b(x, y)\right)\left(N_b - N_a\right) - \frac{N_a}{T_\infty} \right] \tag{3}$$

Eliminating $C_b(x, y)$, the temperature $T(x, y)$ can be calculated by using information from both wave-lengths λ_j and λ_k

$$S_j(x, y) \frac{\lambda_j}{N_{bj} - N_{aj}} - S_k(x,y) \frac{\lambda_k}{N_{bk} - N_{ak}} = \frac{3pl}{2R} \left[\frac{1}{T(x, y)} - \frac{1}{T_\infty} \right] \left[\frac{N_{aj}}{N_{bj} - N_{aj}} - \frac{N_{ak}}{N_{bk} - N_{ak}} \right] \tag{4}$$

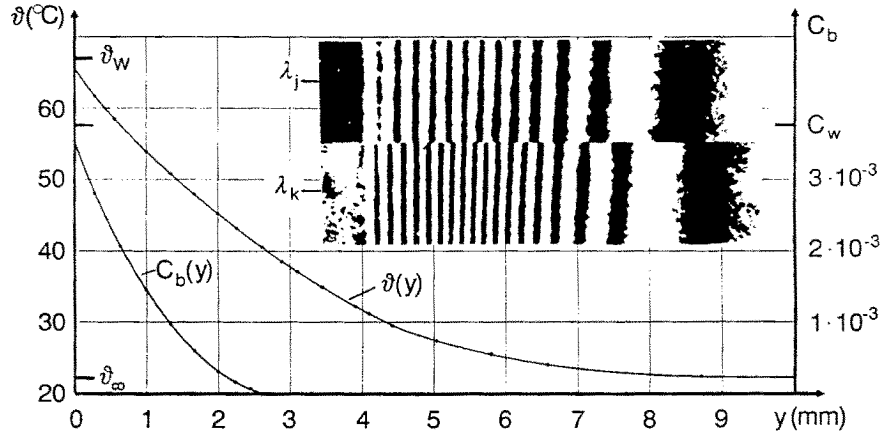

Fig. 18 Two-wavelength interferogram of combined heat and mass transfer by free convection from a vertical plate

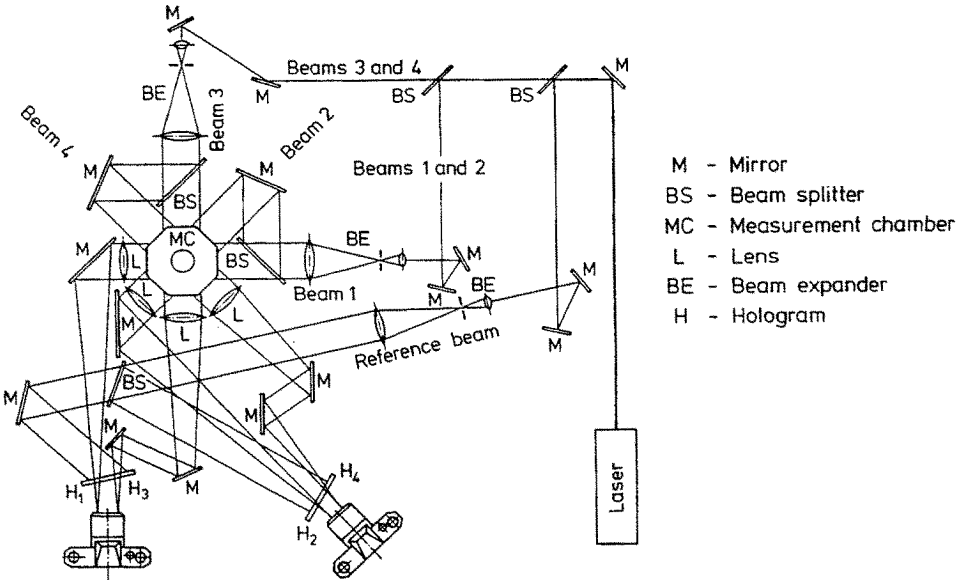

Fig. 19 Optical arrangement for holographic interferometry on a tomographic basis

After determining the temperature distribution, only one interferogram is needed to calculate the concentration profile.

Equation (4) shows that it is the difference between the phase shifts of the two wavelengths that is used for evaluating the temperature. This difference is usually very small. Therefore, the two wavelengths used should be as far apart as possible. The fact that the wavelengths have to be in or near the visible range of light limits the applicability of the method.

A simple example of application for the two-wavelength technique is shown in Fig. 18. A vertical plate was paved with naphthalene and heated. The heat and mass transfer were generated by a natural convective upward air-flow. In order to demonstrate the differences in the phase shift, only the upper and lower halves of each interferogram are shown, and the evaluation is made at the intersection of these two interferograms.

Heat and mass transfer experiments can also be performed in a burning flame as Panknin (1977) demonstrated.

2.3 Interferometric Tomography. The holographic-interferometric methods discussed up to now do not allow us to evaluate a three-dimensional temperature field of complicated local structure, because each beam traveling through the temperature field is integrating all local situations on its way. For a multidimensional information, the volume of interest has to be irradiated from various directions, and a tomographic method can be used to evaluate the various interference patterns and integrate them to a three-dimensional picture.

Figure 19 presents an example of a holographic setup for multidimensional irradiation (Mayinger and Lübbe, 1984; Lübbe, 1982; Ostendorf et al., 1986). The vessel with its volume to be investigated is irradiated via four different object waves spanning an angle of 135 deg. To avoid deflection of the light at curved surfaces of the glass vessel, the outer surrounding of the vessel is arranged in an octagonal form so that each of the beams hits a plain surface in the orthogonal direction. Only the inner vessel is of cylindrical shape. To avoid a deflection of the light at the surface of this inner vessel, a liquid is filled in the annular space between the outer and the inner vessel, which has exactly the same refractive index as the glass of these vessels. After hitting the mirror M, the light of the laser travels to two adjustable beam splitters BS. The first beam splitter fades out the reference wave, and the second beam splitter produces four different object waves, which are expanded via microlenses. A prefocusing of the object waves is produced by four lenses. The arrangement is organized in such a way that it is possible to store two interferograms of high quality on one holographic plate. By proper arrangement of the mir-

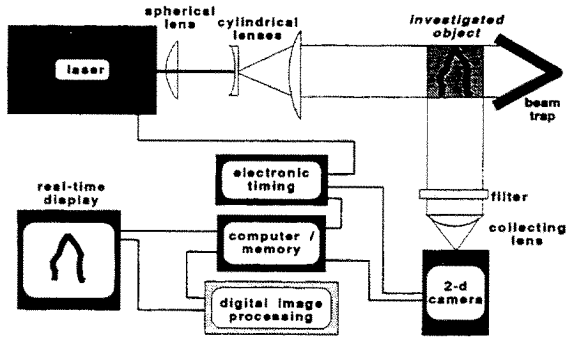

Fig. 20 Experimental arrangement for planar laser-induced fluorescence

Fig. 21 Laser-induced fluorescence (right-hand side) and self-induced fluorescence (left-hand side) from a Bunsen flame

rors, lenses, and beam splitters, it is possible to make the length of the optical paths of the reference waves and of the objects waves almost equal so the demand on the coherence length of the laser can be moderate. The procedure can be combined with real-time holography, and cinematographic recording is also possible.

3 Laser-Induced Fluorescence

Light is comprised of much information and not only the phase shift can be used to get information about the distribution of temperature or concentration in a gas or fluid. Besides the phase shift, the effect of scattering is most commonly used to get information about the chemical and physical conditions of a substance. Raman scattering is a method, which allows us to measure the variety of substances present in a mixture, the concentration of each species, and under certain circumstances also the temperature. Rayleigh scattering can be used as a nonintrusive method for measuring the temperature, and the fluorescence indicates the kind and the density of atoms and molecules and also allows us to deduce the temperature. Of course, there are also other scattering methods, like Mie scattering used in phase-Doppler velocimetry, Bragg scattering for detecting density fluctuations and for investigating the structure of crystals, and Brillouin scattering for measuring sound velocity and sound absorption. Here only the fluorescence used together with a light-sheet method will be discussed, because it is an image-forming process.

The laser-induced fluorescence is based on the fact that when the molecule under investigation is absorbing a photon of the incoming light, the molecule is transferred to a state of higher energy for a short period and falls back to its original energy level when light is emitted. The fluorescence signal determines the type of species via the wavelength, and the intensity of the fluorescence can be used for determining the concentration. Also the temperature of the gas under investigation can be obtained by different techniques, which are based on temperature-dependent equilibrium distribution of the population among the energy levels. This can be done by either exciting different transitions and observing the total light emission or by spectral analysis of the emitted light after broadband excitation. Besides the standard Laser-Induced-Fluorescence (LIF), there has also recently been proposed a slightly altered method in the literature, the Laser-Induced-Predissociation-Fluorescence (LIPF) (Andresen et al., 1988).

The theory about fluorescence is very comprehensive and cannot be discussed in detail here. Therefore, reference is made to the literature (Hanson, 1986, 1990). Here only the experimental setup and the measuring procedure are briefly discussed.

Figure 20 shows an example of a setup for planar fluorescence (LIF) measurements. The laser beam of circular cross section is transformed into a thin light sheet by cylindrical lenses. The thickness of the light sheet determines the spatial resolution and is usually on the order of 100 m. The height of the light sheet depends on the power of the laser and on the format of the camera to be used for observation. A usual value is 50 mm. The light sheet travels through the volume to be investigated. Orthogonal to the light sheet a CCD camera is arranged, which registers the fluorescence induced by the light sheet via a filter and a collecting lens. By using the filter, only the fluorescence signal is observed by the detector in the camera. Usually the solid-state camera is equipped with a gateable image intensifier. The intensity data of the two-dimensional image are transferred from the camera to a data acquisition system, where they are evaluated by a computer. The data are stored in grey scale values, and the resolution capacity depends on the dynamic range of the camera and the intensity of the emitted light. The processed image is finally displayed in false color pictures, where a certain color is associated with a distinct intensity range.

Modern developments in laser and camera technology as well as the modern standard of digital image-processing have led to several LIF applications. Here only one application is presented, namely the investigation of flames, and this example is restricted to hydrogen combustion. To make understanding easier, the flame of a Bunsen burner is investigated. For a better impression, the fluorescence image is compared with a photograph of the glowing flame. The photograph of the left-hand side of Fig. 21 shows only the conical form of the flame and in reality it represents the total fluorescence of the gas produced by the high temperature in the reaction zone. This can be called self-fluorescence. On the right-hand side of Fig. 21, the fluorescence induced by an Excimer laser is registered selectively, monitoring the fluorescence of the OH molecules only, which are emitting light at 308 nm. The laser beam is irradiating a very thin sheet of the flame only, and, therefore, a two-dimensional picture results. The presence of OH indicates the zone of highest reactivity characterizing the center of the flame. The centers of highest reaction are represented by the light zones and spots in the LIF image. The main reaction takes place in a narrow zone near the outer surface of the jet. Due to strong mixing turbulence produced by a flame holder in the center of the mouth of the burner, there are also some high reaction spots in the center of the jet. For a complete, three-dimensional investigation of the flame, the light sheet has to be moved stepwise forward and backward to record the flame layer by layer.

Finally one can combine various optical methods, for example, holographic interferometry and fluorescence to study combustion processes (Mayinger and Haibel, 1992). Figures 22 and 23 present an example of such a combination. The combustion zone of a hydrogen flame was studied in this example, however, under the condition of very high air velocities. The combustion process is controlled by two phenomena, namely the heat and mass transfer and the reaction kinetics. In a diffusion flame, the mass transport usually dominates the combustion. Therefore, this mass transport is of interest at first. It was investigated in a modeling experiment where in-

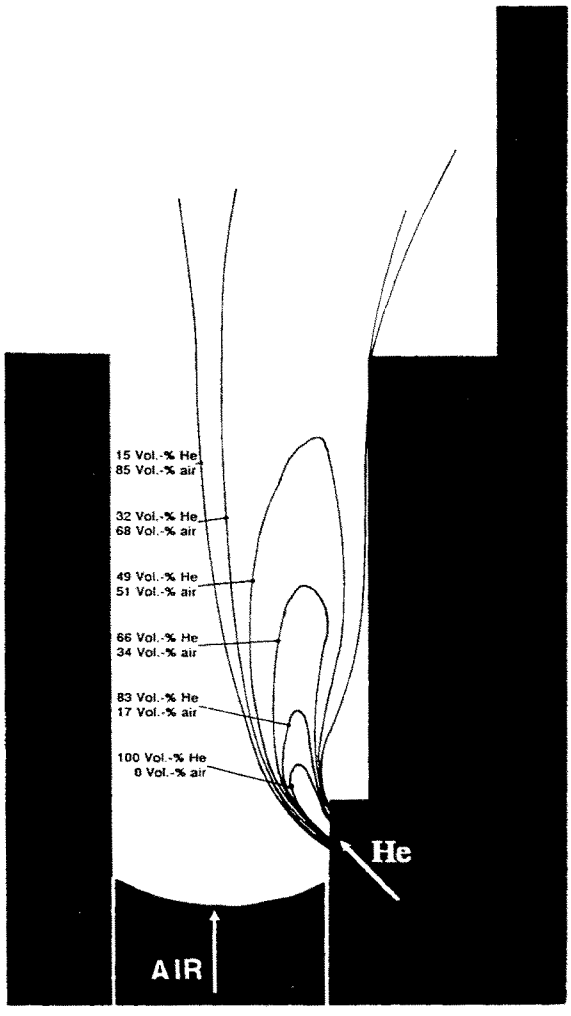

Fig. 22 Concentration distribution in the mixing zone of a high velocity flame; cold experiment with helium as modeling fluid

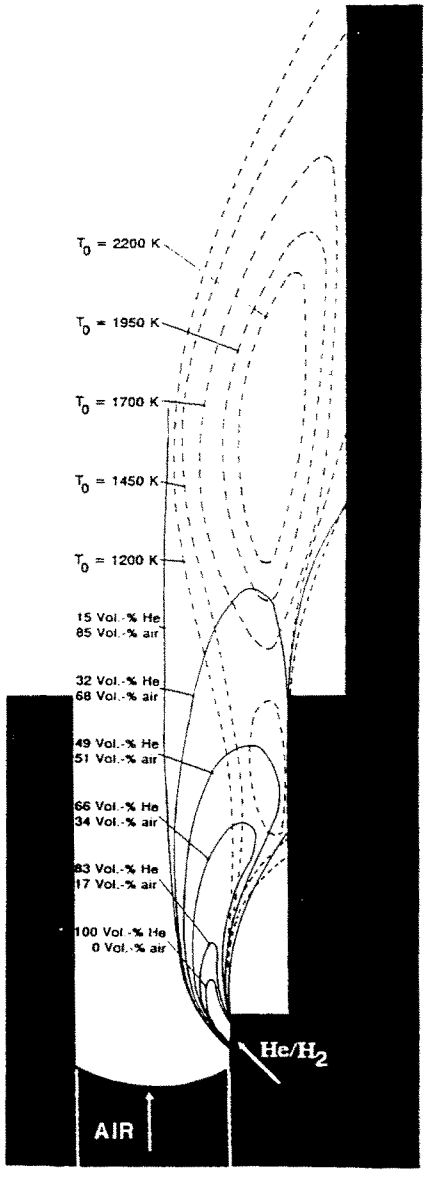

Fig. 23 Readings of the helium mixing experiments superimposed on the isotherms of the burning flame

stead of hydrogen, helium was injected into a high-velocity channel through a tiny nozzle. The concentration of the helium in the channel behind the injection spot was measured by holographic interferometry. The intention was to get a clear insight into the mixing process at first, and, therefore, nonflammable helium was used, having a similar high sound velocity to hydrogen. Figure 22 clearly shows the concentration distribution of the helium in the high velocity air stream.

For a high-speed, high-turbulence flame, the minimum concentration of the fuel must not be too low in order to avoid that the turbulent mixing extinguishing the flame instead of agitating it. One can assume that for a hydrogen flame, a fuel concentration of 10–15 volumetric percent may be a minimum for flame acceleration. Therefore, in Fig. 22 the line of 15 volumetric percent helium can be roughly regarded as the outer border where a high-speed flame can exist.

In Fig. 23 the readings of the helium-mixing experiments are superimposed by isotherms of the burning flame—with hydrogen as fuel—which result from a combined measuring technique of holographic interferometry and a self-induced fluorescence method. The figure clearly conveys the information that the ignition starts in the recirculation zone behind the step in the channel where the air concentration is rather low, but good enough for a first reaction to form radicals like OH. The main combustion takes place far downstream of the spot where the hydrogen was injected, namely in the area where the hydrogen concentration in the air is between 10 and 15 volumetric percent. The superposition of information gained by holographic interferometry and fluorescence proves a good agreement concerning the mixing and the reaction process.

Finally in Fig. 24 it is demonstrated that holographic interferometry not only can register heat and mass transfer processes—like mixing of fuel and air—but also is good for detecting shock fronts in a supersonic flow. In the same channel, as discussed in Figs. 22 and 23, again helium is injected into air, which, however, is now flowing with supersonic velocity upstream of the injection spot. The injection of the fuel not only disturbs the boundary layer, but also displaces the air flow, which finally results in a diagonal compression shock, starting at the boundary between mixing zone and undisturbed air flow downstream of the injection spot. In Fig. 24 the finite fringe method was used, and, therefore, parallel oriented fringes indicate none or weakly influenced air flow.

4 Concluding Remarks

Optical methods are expected to experience a powerful revival due to three reasons:

Sophisticated theoretical treatment of heat and mass transfer processes with large computer codes needs very detailed in-

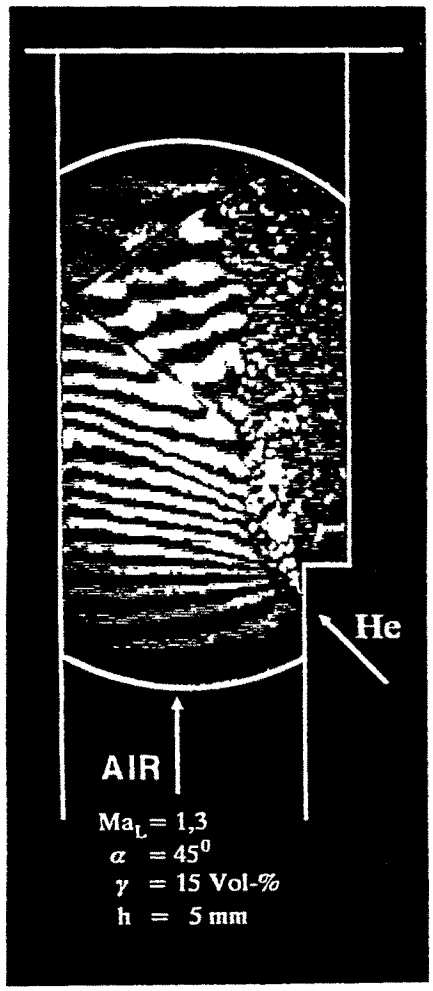

Fig. 24 Interferogram of mixing jet with a shock front in a Laval nozzle

formation about temperature and concentration fields in the area of interest for accessing and improving the physical models used in codes and for verifying such codes. An optically determined pattern of isotherms is a very stringent touchstone for the reliability and accuracy of a code.

Modern developments in power and process engineering make transient situations more and more interesting, especially for controlling procedures and safety deliberations. Optical measuring techniques work inertia-less and nonintrusively.

A former drawback of the image-forming optical measuring techniques, the laborious and time-consuming evaluation, does not exist anymore. Even a personal computer is good enough for evaluating a hologram or an interferogram within a few seconds, a process that took several hours in the past. The costs of such an evaluating equipment are relatively moderate.

A new symbiosis could come into being between theorists and experimentalists, working in heat and mass transfer.

References

Andresen, P., Bath, A., Gröger, W., Lülf, H. W., Meijer, G., and ter Meulen, J. J., 1988, "Laser-Induced Fluorescence With Tunable Excimer Lasers as a Possible Method for Instantaneous Temperature Field Measurements at High Pressures: Check With an Atmospheric Flame," *Appl. Optics*, Vol. 27(2), p. 365.

Caulfield, H. J., and Lu, Sun, 1971, *The Applications of Holography*, Wiley Interscience, New York.

Chavez, A., and Mayinger, F., 1990, "Evaluation of Pulsed Laser Holograms of Spray Droplets by Applying Image Processing," *9th International Conference on Heat Transfer*, p. 187.

Chavez, A. A., 1991, "Holografische Untersuchung an Einspritzstrahlen—Fluiddynamik und Wärmeübertragung durch Kondensation," Diss. Techn. Univ. München, Federal Republic of Germany.

Chavez, A., and Mayinger, F., 1992, "Measurement of Direct-Contact Condensation of Pure Saturated Vapour on an Injection Spray by Applying Pulsed Laser Holography," *Int. J. Heat Mass Transfer*, Vol. 35, No. 3, pp. 691–702.

Chen, Y. M., 1985, "Wärmeübertragung an der Phasengrenze kondensierender Blasen," Diss. Techn. Univ. München, Federal Republic of Germany.

El-Wakil, X. X., Myers, G. E., and Schilling, R. J., 1966, "An Interferometric Study of Mass Transfer From a Vertical Plate at Low Reynolds Numbers," ASME JOURNAL OF HEAT TRANSFER, Vol. 88, pp. 399–406.

Hanson, R. K., 1986, "Combustion Diagnostics: Planar Imaging Techniques, *18th Symp. (Intl.) on Combustion*, The Combustion Institute, Pittsburgh, PA.

Hanson, R. K., Seitzmann, J. M., and Paul, P. H., 1990, "Planar Fluorescence Imaging of Gases," *Applied Physics*, Vol. B50, pp. 441–454.

Hauf, W., and Grigull, U., 1970, "Optical Methods in Heat Transfer," *Advances in Heat Transfer*, Vol. 6, p. 133.

Hauf, W., 1991, "Das Mach-Zehnder-Interferometer," in: *Optische Meßverfahren in der Wärme- und Stoffübertragung*, U. Grigull, ed., Springer-Verlag, Berlin, pp. 70–130.

Kiemle, H., and Röss, D., 1969, *Einführung in die Technik der Holographie*, Akademische Verlagsgesellschaft, Frankfurt, Federal Republic of Germany.

Klas, J., 1993, "Wärmeübertragung in Strömungskanälen ohne und mit Turbulenzpromotoren," Diss. Techn. Univ. München, Federal Republic of Germany.

Lighthart, G., and Groen, C. A., 1982, "A Comparison of Different Autofocus Algorithms," *IEEE Trans.*, Vol. XX, pp. 597–604.

Lübbe, D., 1982, "Ein Messverfahren für instationäre dreidimensionale Verteilungen und seine Anwendung auf Mischvorgänge," Diss. Universität Hannover, Federal Republic of Germany.

Mayinger, F., and Panknin, W., 1974, "Holography in Heat and Mass Transfer," *5th Int. Heat Transfer Conference*, Tokyo, Vol. VI, p. 28.

Mayinger, F., and Lübbe, D., 1984, "Ein tomographisches Messverfahren und seine Anwendung auf Mischvorgänge und Stoffaustausch. 2," *Wärme- und Stoffübertragung*, Vol. 18, pp. 49–59.

Mayinger, F., 1991, "Holographie und holographische Interferometrie in Optische Meßverfahren in der Wärme- und Stoffübertragung," U. Grigill, ed., Springer-Verlag, Berlin, pp. 194–225.

Mayinger, F., and Haibel, M., 1992, "Turbulenz-gestützte Gemischbildung und Stabilisierung von sub- und supersonischen Wasserstoff-Luft-Flammen," *DGLR-Jahrbuch*, Bremen, Federal Republic of Germany.

Ostendorf, W., Mewes, D., and Mayinger, F., 1986, "A Tomographical Method Using Holographic Interferometry for the Registration of Three-Dimensional Unsteady Temperature Profiles in Laminar and Turbulent Flow," *Heat Transfer 1986, Proc. of the 8th Int. Heat Transfer Conference*, C. L. Tiens, et al., eds., Hemisphere Publ. Corp., New York, Vol. 2, pp. 519–524.

Panknin, W., 1977, "Eine holographische Zweiwellenlängen-Interferometrie zur Messung überlagerter Temperatur- und Konzentrationsgrenzschichten," Ph.D. thesis, Techn. Universität Hannover, Federal Republic of Germany.

Panknin, W., and Mayinger, F., 1978, "Anwendung der holographischen Zweiwellenlängen-interferometrie zur Messung überlagerter Temperatur- und Konzentrationsgrenzschichten," *Verfahrenstechnik*, Vol. 12, No. 9, pp. 582–589.

Smith, H. M., 1969, *Principles of Holography*, Wiley, New York.